Organometallic Nanowires

DOI: 10.1002/anie.200802981

Semiconducting and Electroluminescent Nanowires Self-Assembled from Organoplatinum(II) Complexes**

*Mai-Yan Yuen, V. A. L. Roy, Wei Lu, Steven C. F. Kui, Glenna So Ming Tong, Man-Ho So, Stephen Sin-Yin Chui, Michele Muccini, J. Q. Ning, S. J. Xu, and Chi-Ming Che**

One-dimensional (1D) nanostructures such as nanowires and nanotubes have inspired much research interest because of their unique electronic and optical properties.[1] In this area, there is a considerable interest in assembling semiconducting nanowires from small organic or organometallic molecules, which not only serve as low-cost and high-performance building blocks for device fabrication, but also possess structural tailorability and multifunctionality.[2,3] Recent advances in molecular electronics have revealed that luminescent organic and organometallic complexes can be used to fabricate organic light-emitting field-effect transistors (OLEFETs).[4]

Luminescent platinum(II) complexes with chelating π-conjugated ligands have engendered widespread interest[5] because of their intriguing structural and spectroscopic properties.[6] We and others have demonstrated that 1) intermolecular $Pt^{II}\cdots Pt^{II}$ or ligand–ligand interactions can facilitate anisotropic growth of 1D nanomaterials with luminescent properties[7] or current-modulating functionality;[8] and 2) various neutral platinum(II) complexes can be used as electrophosphorescent dopants for high-performance organic light-emitting diodes (OLEDs).[9] We thus envisage that it may be feasible to develop OLEFETs by incorporating switching and photoluminescent properties of platinum(II) nanostructures into a single compact device. Herein we report self-assembled organoplatinum(II) nanowires and their electroluminescent and ambipolar semiconducting properties.

In this work, we chose cationic cyclometalated/terpyridyl platinum(II) complexes (**1**–**9**) bearing arylisocyanide/arylacetylide ligands by taking into consideration the following

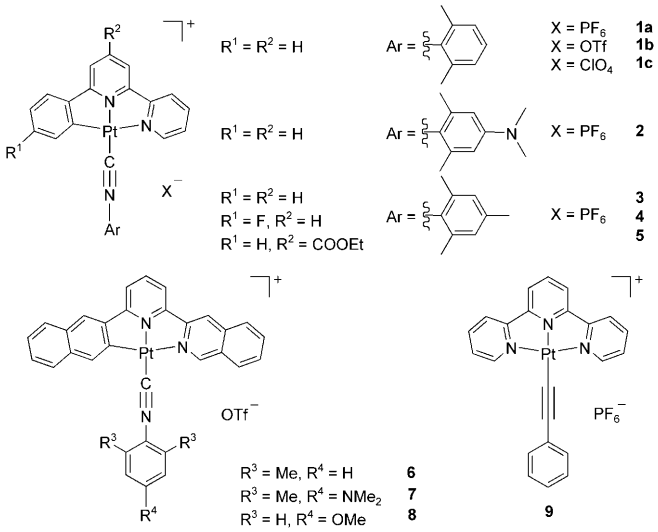

criteria: 1) they have highly emissive triplet metal-to-ligand charge-transfer (MLCT) or metal-metal-to-ligand charge-transfer (MMLCT) excited states in solution and in the solid state;[10] 2) molecular aggregation through $Pt^{II}\cdots Pt^{II}$ or ligand–ligand interactions is significant for these two classes of planar platinum(II) complexes;[11] and 3) the negatively charged counterions are anticipated to be transported towards the anode upon a biased electrical field and may aid charge injection during the operation of a light-emitting transistor.[12] Furthermore, complexes **6**–**8** are robust towards moisture, air, and light irradiation, and exhibit high emission quantum yields.[13]

Complexes **1**–**8** were prepared by a simple ligand substitution reaction of the corresponding cyclometalated platinum(II) chloride precursor with arylisocyanide.[10a] Complex **9** was prepared according to reported procedures.[10b] Crystal structures of **1a**·CH_3CN[11a] and **9**·CH_3CN[10b] have previously been reported. We were able to determine the crystal structure of a needle-like crystal of **1a**·H_2O, which was obtained by slow evaporation in 1:1 CH_3CN/H_2O (v/v). The salient feature of the crystal structure of **1a**·H_2O is the infinite $Pt^{II}\cdots Pt^{II}$ chains along the *c* axis with alternate intermetal separations of 3.382(2) and 3.344(2) Å (Figure 1), similar to

[*] M.-Y. Yuen,[+] Dr. V. A. L. Roy,[+] Dr. W. Lu, Dr. S. C. F. Kui, Dr. G. S. M. Tong, M.-H. So, Dr. S. S.-Y. Chui, Prof. C.-M. Che
Department of Chemistry and HKU-CAS Joint Laboratory on New Materials, The University of Hong Kong, Pokfulam Road, Hong Kong (China)
E-mail: cmche@hku.hk
Homepage: http://chem.hku.hk/~chemhome/staff/cmche/cmche.htm
Dr. M. Muccini
CNR-ISMN, Istituto per lo Studio dei Materiali Nanostrutturati, Bologna (Italy)
J. Q. Ning, Dr. S. J. Xu
Department of Physics, The University of Hong Kong (China)
[+] These authors contributed equally to this work.

[**] This work is supported by the University Development Fund of the University of Hong Kong, the Hong Kong Research Grants Council (HKU 7039/03P), the Italian FIRB-RBNE033KMA, and the EUFP6-015034O LAS projects. We are grateful to Dr. Herman H. Y. Sung of the Hong Kong University of Science and Technology for performing the low-temperature X-ray crystallography on **1a**·H_2O and S. Toffanin of CNR-ISMN for CLSM measurements.

Supporting information for this article is available on the WWW under http://dx.doi.org/10.1002/anie.200802981.

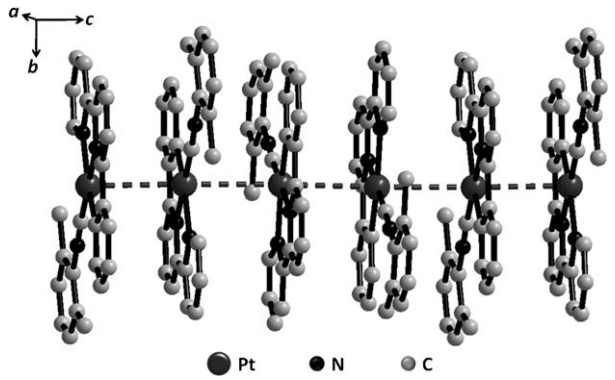

Figure 1. Crystal packing diagram of **1a**·H_2O. The PF_6^- counterions and disordered water molecules are omitted for clarity.

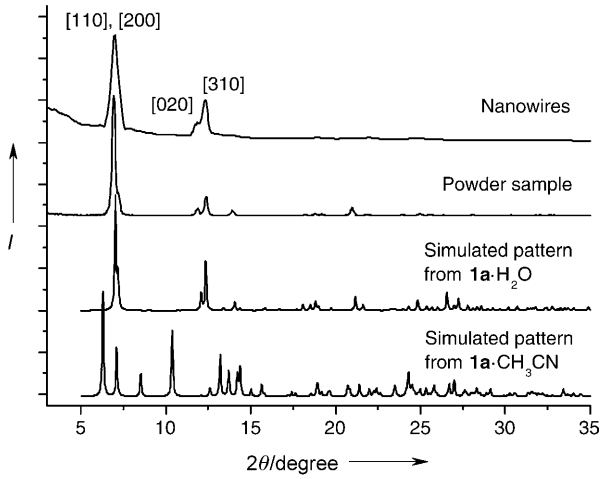

Figure 2. Powder XRD patterns of **1a**: as-prepared nanowires (top), powder sample (middle), and simulated patterns from crystallographic data of **1a**·H_2O and **1a**·CH_3CN (bottom).

that of **9**·CH_3CN.[11a] These $Pt^{II}\cdots Pt^{II}$ distances are shorter than the sum of van der Waals radii (3.44 Å), indicating extended $d^8\cdots d^8$ interactions in the solid state. The uniform Pt-Pt-Pt angles of 178.71(2)° reveal the linear nature of the $Pt^{II}\cdots Pt^{II}$ backbone. The chelated platinum(II) moiety and the arylisocyanide ligand are coplanar, and this cationic plane is roughly perpendicular to the *c* axis. There are two alternate C(isocyanide)-Pt-Pt-C(isocyanide) torsion angles (111.8° and 180.0°) between two neighboring cations along the $Pt^{II}\cdots Pt^{II}$ backbone. We note that the crystal structure of **1a**·H_2O is different from that of **1a**·CH_3CN.[10b] In the latter case, no infinite $Pt^{II}\cdots Pt^{II}$ chains but rather head-to-tail pairs with an intermetal separation of 3.384 Å were found for the cations of **1a**.

The precipitation method was adopted to prepare the nanowires. We use **1a**, **6**, and **9** as representative examples in the following description. The complex was first dissolved in acetonitrile to give a bright yellow solution (ca. 1.0 mM, 100 μL). Nanowires were obtained as a virtually transparent purple, orange, or green dispersion for **1**, **6**, and **9**, respectively, by injecting the acetonitrile solution into deionized water (1000 μL). Nanowires were collected by centrifugation and redispersed in deionized water three times. Removal of organic solvent from the aqueous dispersion was found to be crucial to prevent further aggregation and growth of the nanowires. The as-prepared aqueous dispersions of nanowires were macroscopically homogeneous and stable for a few weeks under ambient conditions.

The powder X-ray diffraction (XRD) pattern of a dried film of nanowire **1a** was compared with those simulated from the crystal data of **1a**·H_2O and **1a**·CH_3CN (Figure 2). The packing of molecules in the nanowires resembled that in the crystal form **1a**·H_2O but not that in **1a**·CH_3CN. The diffraction peaks at $2\theta = 6.98$, 7.19, 12.08, and 12.26° ($d =$ 12.65, 12.28, 7.32, and 7.21 Å, respectively) are prominent in the XRD pattern of the nanowires and could be indexed as the Miller planes [110], [200], [020], and [310] of the X-ray crystal structure of **1a**·H_2O. Since the XRD pattern of the nanowires did not show diffraction peaks associated to the Miller planes [00*l*] of the crystal structure, the cations of **1a** might preferentially aggregate together along the long axis of the nanowires through intermolecular $Pt^{II}\cdots Pt^{II}$ interactions.

Transmission electron microscopy (TEM, Figure 3a) and scanning electron microscopy (SEM, Figure 3c) images confirmed the 1D nature of nanowires of **1a**. The elements present in the nanowires were confirmed by energy-dispersive X-ray (EDX) spectroscopy (for details see Figure S2 in the Supporting Information). The average diameter of the nanowires was 25 ± 3 nm with a monodispersity of 12.4%. The

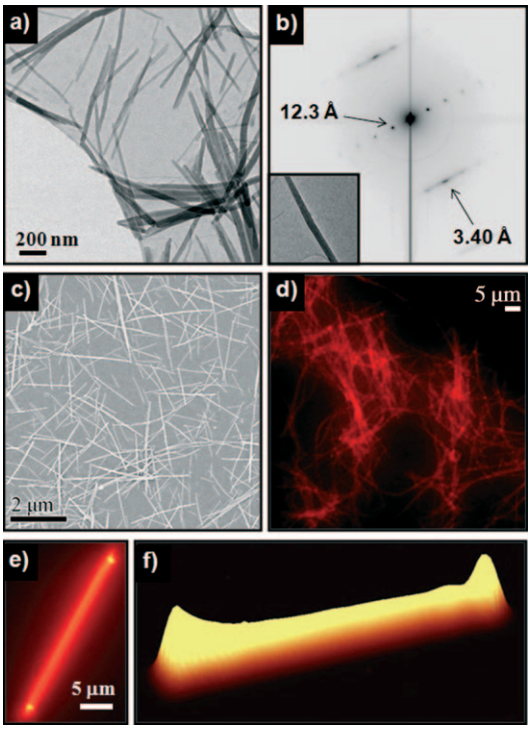

Figure 3. Microscopic studies: a) TEM image; b) SAED pattern (inset shows the TEM image of the corresponding single nanowire that has been rotated 92° to compensate the image-diffraction pattern rotational angles so that the diffraction pattern coincides in orientation with the shown nanowire); c) SEM image; and d) fluorescence micrograph (upon excitation at 550 nm) of the nanowires prepared with **1a**. e) CLSM micrograph and f) spatially resolved 3D emission intensity (in arbitrary units) of a single submicrometer wire prepared with **6**.

length of the nanowires spanned from 2.0 to 3.5 μm with an average value of 2.2 μm. No significant changes in morphology were observed upon changing the counterion from PF_6^- to $CF_3SO_3^-$ or ClO_4^-. Submicrometer wires of **6** prepared with the same procedure as **1a** were found to have much larger diameters of 253 ± 54 nm and a longer average length of 3.8 μm. Presumably this difference is due to the lower solubility of **6** in CH_3CN, so that large molecular aggregates of **6** could be formed upon addition of H_2O. Nanowires **9** have an average diameter 27 ± 4 nm and length of 1.0–1.5 μm.

Sharp and ordered spots were observed in the selected area electron diffraction (SAED) pattern of a single nanowire of **1a** (Figure 3b). The *d* spacings of 12.3 and 3.40 Å correspond to the respective [200] and [004] Miller planes found in the crystal structure of **1a**·H_2O. On the basis of the X-ray and electron diffraction data, the growth direction of the nanowires coincides with the *c* axis, that is, along the long axis of $Pt^{II}\cdots Pt^{II}$ chains. We suggest that $Pt^{II}\cdots Pt^{II}$ interaction directs the anisotropic growth of these nanowires.

UV/Vis reflectance spectra were recorded for films prepared by drop-casting aqueous dispersions of nanowires onto a silicon substrate. Nanowires **1a**–**1c**, **6**, and **9** showed low-energy reflectance bands at λ_{max} = 584 (**1a**), 534 (**1b**), 592 (**1c**), 528 (**6**), and 652 (**9**) nm (for representative spectra, see Figure 4, left), and intense red to near-infrared (NIR)

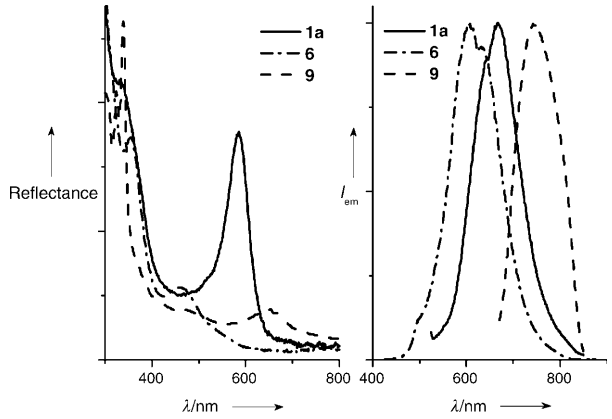

Figure 4. UV/Vis reflectance (left) and emission (right) spectra of nanowires **1a**, **6**, and **9**.

emission at λ_{max} 668 (**1a**), 614 (**1b**), 679 (**1c**), 607 (**6**), and 742 (**9**) nm (for representative spectra, see Figure 4, right). Saturated red emission from the segregated nanowires of **1a** was observed directly under a fluorescence microscope with an excitation wavelength of 550 nm (Figure 3d). Upon laser excitation at 488 nm and viewed under a confocal laser scanning microscope (CLSM), submicrometer wire of **6** exhibited an orange emission with bright spots at both ends of the wire and a weaker emission observed from the wire body (Figure 3e). The spatially resolved three-dimensional image of the edge emission from a single submicrometer wire of **6** (Figure 3f) showed two distinct peaks at both ends of the wire. This result is typical for an optical waveguide,[14] revealing that the wires of **6** are able to absorb excitation light and propagate the light emission towards the tips.

We take **1a**, **6**, and **9** as representative examples to discuss the spectroscopic properties (see Table S5 in the Supporting Information for absorption and emission data). Upon excitation at $\lambda > 350$ nm, **1** and **9** show a structureless emission band at λ_{max} = 527 and 630 nm (lifetimes in microsecond regime),[10b] respectively, in acetonitrile at 298 K (Figure S3 in the Supporting Information); these bands are blue-shifted from those for nanowires **1a** (λ_{max} = 668 nm) and **9** (λ_{max} = 742 nm). By reference to previous works,[10,11] the low-energy emissions from nanowires **1a** and **9** can be assigned to MMLCT excited states. This assignment is supported by the presence of $Pt^{II}\cdots Pt^{II}$ interactions in the nanowires. A 4×10^{-5} M solution of **6** in acetonitrile shows a vibronically structured emission band with peak maxima at λ_{max} = 512, 553, and 611 nm and a lifetime of around 10 μs, whereas structureless emission at λ_{max} = 632 nm was observed at a higher complex concentration of 4×10^{-4} M (Figure S11 in the Supporting Information). We ascribe the high-energy emission at 510–611 nm to a triplet excited state with mixed ^{3}IL/^{3}MLCT [(5d)Pt→π*(chelated ligand)] character. The emissions at $\lambda_{max} > 600$ nm found with **6** at high concentrations and with nanowires of **6** are assigned to excimeric $^3(\pi\text{–}\pi^*)$ excited states.

Studies on the semiconducting and electroluminescent properties of these self-assembled nanowires were conducted by using a bottom-contact FET configuration. Aqueous dispersions of nanowires **1**, **6**, and **9** were drop-cast on the top of patterned SiO_2 substrates. Figure 5 (top) shows the output characteristics (I_{DS} versus V_{GS} at different V_{DS} values) as well as the electroluminescence intensity from the bottom-contact OLEFET device with nanowires of **1a** as an active layer after annealing at 350 K. The drain-source current I_{DS} increased with increasing both positive and negative gate voltage, indicating ambipolar behavior of the field-effect transistor. The field effect was found to be dependent on the annealing temperature. An increase in current intensity and up to three orders of magnitude enhancement of field-effect mobility were identified for annealed film when compared with the non-annealed sample. The highest mobility was achieved at an annealing temperature of 350 K (Table 1); thus, all following results were obtained by using such annealed nanowires. This remarkable enhancement in mobility was consistent with the formation of larger crystal domains observed upon annealing (see Figure S24 in the Supporting Information for SEM micrographs of the film before and after annealing), which was anticipated to decrease the crystal grain boundary.[15] The complex anion did not significantly affect the device performance, as the devices prepared from nanowires **1a**–**c** exhibited comparable electron and hole mobilities. We found that nanowires and submicromater wires of **1**, **6**, and **9** behave as ambipolar semiconductors with both hole and electron mobility around 0.1 $cm^2V^{-1}s^{-1}$ (Table 1), which are comparable to those of ambipolar semiconductors derived from acenes and thiophenes.[16]

Single-point energy calculations on the monomeric and dimeric structures of both **1a** and **9** with the geometries taken from their respective crystal structures were performed with

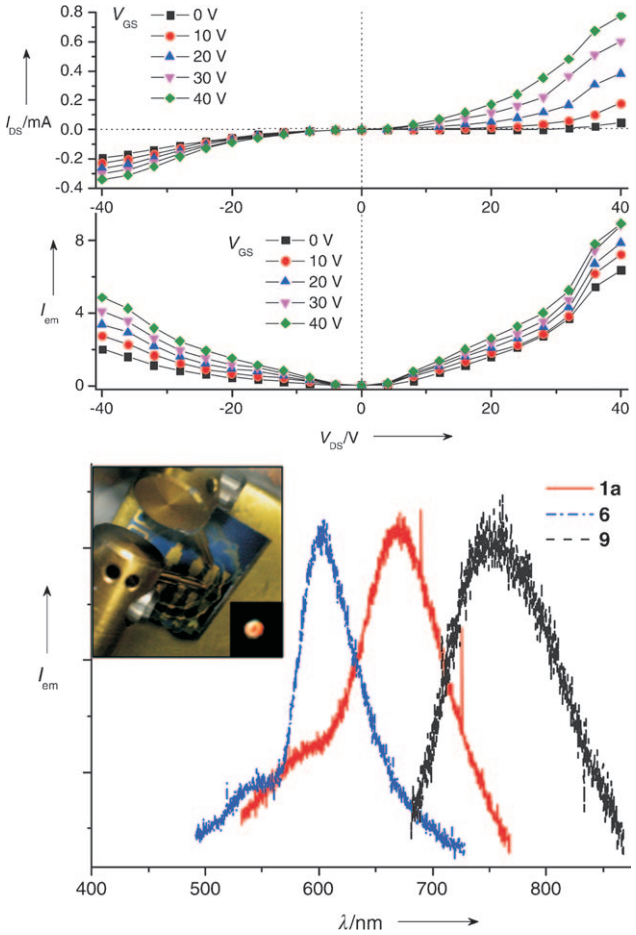

Figure 5. Top: Output characteristics (I_{DS} vs. V_{DS}) and electroluminescence intensity (I) of an OLEFET device made up of nanowires **1a** after annealing at 350 K. Bottom: Normalized electroluminescence spectra of OLEFET device with nanowires of **1a**, **6**, and **9** as active materials. Inset shows images of a real device and the observed electroluminescence from wires of **6** during the device operation.

Table 1: Field-effect mobilities of nanowires **1**, **6**, and **9** before and after annealing at 350 K under vacuum (10^{-4} Torr). Charge mobilities (μ_h and μ_e) were calculated at the linear regime ($V_{DS} \ll V_G$).

Nanowire	μ_h [$cm^2V^{-1}s^{-1}$]		μ_e [$cm^2V^{-1}s^{-1}$]	
	Before annealing	After annealing	Before annealing	After annealing
1a	10^{-4}	0.15	10^{-3}	0.20
1b	10^{-4}	0.08	10^{-4}	0.10
1c	10^{-4}	0.10	10^{-5}	0.20
6	10^{-4}	0.09	10^{-3}	0.16
9	10^{-4}	0.10	10^{-3}	0.18

density functional theory (DFT) (see the Supporting Information for details). The calculated LUMO energies for monomers **1a** (−3.91 eV) and **9** (−4.06 eV) are similar. The calculated HOMO energy is significantly more negative for monomer **1a** (−7.54 eV) than for monomer **9** (−6.52 eV). With Au as the source/drain electrode, the electron injection barriers (0.9–1.1 eV) are smaller than the hole injection barriers (1.5–2.5 eV) for both **1a** and **9**, which is in good correlation with the electron mobility being an order of magnitude larger than the hole mobility for both **1a** and **9** before annealing (Table 1). The calculated HOMO–LUMO energy gaps of dimeric **9** (2.59–2.67 eV) are smaller than those of dimeric **1a** (3.44–3.69 eV). This result is consistent with the finding that nanowire **9** has a lower emission energy than nanowire **1a**. There are two stacking arrangements for both dimeric **1a** and **9**, namely, head-to-tail and skewed. The splitting calculations revealed that the hole-transfer integral is significantly larger than the electron-transfer integral for both head-to-tail and skewed forms of dimeric **1a**, and is more than an order of magnitude larger than the hole transfer integrals for both forms of dimeric **9**. On the basis of the splitting calculations for the dimeric structures, holes should be the major charge carrier for **1a**. For **9**, depending on the stacking arrangement, the charge carriers could either be ambipolar in the head-to-tail form or mainly electron-based in the skewed form. As our calculation has not included the reorganization energy, which is also important in determining the charge mobility, the apparently similar hole and electron mobilities for nanowires of **1a** and **9** after annealing could be due to morphological changes of the complexes at high temperatures, which could affect the size of the charge-transfer integrals. The explicit role of anions in the charge-injection process has not yet been evaluated from these theoretical calculations. There is a delicate interplay between the charge-transfer characteristics and the charge injection barriers in the evaluation of the performance of such systems, and further studies are necessary for better understanding of the semiconducting properties of these nanostructured platinum(II) complexes.

Electroluminescence was observed in both the positive and negative gate bias. The intensity of the light emission from these devices increased with increasing gate voltages (Figure 5, top). Electroluminescent spectra for OLEFET devices with nanowires of **1a**, **6**, and **9** as active materials are depicted in Figure 5 (bottom). The electroluminescence peak maximum is at 669, 603, and 755 nm for devices fabricated with nanowires of **1a**, **6**, and **9**, respectively. These peak maxima are similar in energy to the respective photoluminescence ($\lambda_{em} = 668$ nm for nanowire **1a**, 607 nm for nanowire **6**, and 742 nm for nanowire **9**). In addition, shoulders at approximately 540 and 590 nm were observed for nanowires **1a** and **6**, respectively, in the electroluminescence spectra. The most possible origin for these high-energy emission shoulders is monomeric MLCT excited states of complexes **1a** and **6**.

In conclusion, we have demonstrated that crystalline, waveguiding, semiconducting, and electroluminescent nanowires can be self-assembled from molecular organoplatinum(II) complexes through extended intermolecular $Pt^{II}\cdots Pt^{II}$ or ligand–ligand interactions. Ambipolar OLEFET devices emitting in the red or NIR region have been fabricated with a solution-processible protocol.

Received: June 22, 2008
Revised: September 5, 2008
Published online: November 12, 2008

Keywords: luminescence · metal–metal interactions · nanostructures · platinum · semiconductors

[1] a) J. T. Hu, T. W. Odom, C. M. Lieber, *Acc. Chem. Res.* **1999**, *32*, 435 – 445; b) Y. N. Xia, P. D. Yang, Y. G. Sun, Y. Y. Wu, B. Mayers, B. Gates, Y. D. Yin, F. Kim, H. Q. Yan, *Adv. Mater.* **2003**, *15*, 353 – 389; c) Y. Ding, Z. L. Wang, *J. Phys. Chem. B* **2004**, *108*, 12280 – 12291.

[2] a) A. P. H. J. Schenning, E. W. Meijer, *Chem. Commun.* **2005**, 3245 – 3258; b) J. A. A. W. Elemans, R. van Hameren, R. J. M. Nolte, A. E. Rowan, *Adv. Mater.* **2006**, *18*, 1251 – 1266.

[3] For examples, see: a) M. Enomoto, A. Kishimura, T. Aida, *J. Am. Chem. Soc.* **2001**, *123*, 5608 – 5609; b) J. J. Chiu, C. C. Kei, T. P. Perng, W. S. Wang, *Adv. Mater.* **2003**, *15*, 1361 – 1364; c) Z. C. Wang, C. J. Medforth, J. A. Shelnutt, *J. Am. Chem. Soc.* **2004**, *126*, 15954 – 15955; d) H. B. Liu, Q. Zhao, Y. L. Li, Y. Liu, F. S. Lu, J. P. Zhuang, S. Wang, L. Jiang, D. B. Zhu, D. P. Yu, L. F. Chi, *J. Am. Chem. Soc.* **2005**, *127*, 1120 – 1121; e) Y. J. Li, X. F. Li, Y. L. Li, H. B. Liu, S. Wang, H. Y. Gan, J. B. Li, N. Wang, X. R. He, D. B. Zhu, *Angew. Chem.* **2006**, *118*, 3721 – 3725; *Angew. Chem. Int. Ed.* **2006**, *45*, 3639 – 3643; f) J. Puigmartí-Luis, A. Minoia, A. P. del Pino, G. Ujaque, C. Rovira, A. Lledos, R. Lazzaróni, D. B. Amabilino, *Chem. Eur. J.* **2006**, *12*, 9161 – 9175; g) X. R. He, Q. K. Li, Y. L. Li, N. Wang, Y. B. Song, X. F. Liu, M. J. Yuan, W. Xu, H. B. Liu, S. Wang, Z. G Shuai, D. B. Zhu, *J. Phys. Chem. B* **2007**, *111*, 8063 – 8068.

[4] First OLEFET: a) A. Hepp, H. Heil, W. Weise, M. Ahles, R. Schmechel, H. von Seggern, *Phys. Rev. Lett.* **2003**, *91*, 157406; for reviews, see: b) M. Muccini, *Nat. Mater.* **2006**, *5*, 605 – 613; c) J. Zaumseil, H. Sirringhaus, *Chem. Rev.* **2007**, *107*, 1296 – 1323; d) F. Cicoira, C. Santato, *Adv. Funct. Mater.* **2007**, *17*, 3421 – 3434.

[5] S. W. Lai, C. M. Che, *Top. Curr. Chem.* **2004**, *241*, 27 – 63.

[6] a) G. Gliemann, H. Yersin, *Struct. Bonding (Berlin)* **1985**, *62*, 87 – 153; b) D. M. Roundhill, H. B. Gray, C. M. Che, *Acc. Chem. Res.* **1989**, *22*, 55 – 61; c) V. M. Miskowski, V. H. Houlding, *Inorg. Chem.* **1991**, *30*, 4446 – 4452.

[7] a) Y. H. Sun, K. Q. Ye, H. Y. Zhang, J. H. Zhang, L. Zhao, B. Li, G. D. Yang, B. Yang, Y. Wang, S. W. Lai, C. M. Che, *Angew. Chem.* **2006**, *118*, 5738 – 5741; *Angew. Chem. Int. Ed.* **2006**, *45*, 5610 – 5613; b) F. Camerel, R. Ziessel, B. Donnio, C. Bourgogne, D. Guillon, M. Schmutz, C. Iacovita, J. P. Bucher, *Angew. Chem.* **2007**, *119*, 2713 – 2716; *Angew. Chem. Int. Ed.* **2007**, *46*, 2659 – 2662; c) A. Y. Y. Tam, K. M. C. Wong, G. X. Wang, V. W. W. Yam, *Chem. Commun.* **2007**, 2028 – 2030; d) W. Lu, Y. C. Law, J. Han, S. S. Y. Chui, D. L. Ma, N. Y. Zhu, C. M. Che, *Chem. Asian J.* **2008**, *3*, 59 – 69; e) W. Lu, S. S. Y. Chui, K. M. Ng, C. M. Che, *Angew. Chem.* **2008**, *120*, 4644 – 4648; *Angew. Chem. Int. Ed.* **2008**, *47*, 4568 – 4572.

[8] W. Lu, V. A. L. Roy, C. M. Che, *Chem. Commun.* **2006**, 3972 – 3974.

[9] a) W. Lu, B. X. Mi, M. C. W. Chan, Z. Hui, N. Zhu, S. T. Lee, C. M. Che, *Chem. Commun.* **2002**, *126*, 206 – 207; b) V. Adamovich, J. Brooks, A. Tamayo, A. M. Alexander, P. I. Djurovich, B. W. D'Andrade, C. Adachi, S. R. Forrest, M. E. Thompson, *New J. Chem.* **2002**, *26*, 1171 – 1178; c) M. Cocchi, D. Virgili, V. Fattori, D. L. Rochester, J. A. G. Williams, *Adv. Funct. Mater.* **2007**, *17*, 285 – 289.

[10] a) S. W. Lai, M. C. W. Chan, K. K. Cheung, C. M. Che, *Organometallics* **1999**, *18*, 3327 – 3336; b) V. W. W. Yam, R. P. L. Tang, K. M. C. Wong, K. K. Cheung, *Organometallics* **2001**, *20*, 4476 – 4482.

[11] a) S. W. Lai, H. W. Lam, W. Lu, K. K. Cheung, C. M. Che, *Organometallics* **2002**, *21*, 226 – 234; b) V. W. W. Yam, K. M. C. Wong, N. Zhu, *J. Am. Chem. Soc.* **2002**, *124*, 6506 – 6507.

[12] For ionic transistors, see: a) X. L. Chen, Z. Bao, J. H. Schön, A. J. Lovinger, Y.-Y. Lin, B. Crone, A. Dodabalapur, B. Batlogg, *Appl. Phys. Lett.* **2001**, *78*, 228 – 230; b) J. Locklin, K. Shinbo, K. Onishi, F. Kaneko, Z. Bao, R. C. Advincula, *Chem. Mater.* **2003**, *15*, 1404 – 1412; c) A. Hepp, H. Heil, R. Schmechel, H. Von Seggern, *Adv. Eng. Mater.* **2005**, *7*, 957 – 960.

[13] S. C. F. Kui, I. H. T. Sham, C. C. C. Cheung, H. W. Ma, B. P. Yan, N. Y. Zhu, C. M. Che, W. F. Fu, *Chem. Eur. J.* **2007**, *13*, 417 – 435.

[14] a) D. O'Carroll, I. Lieberwirth, G. Redmond, *Nat. Nanotechnol.* **2007**, *2*, 180 – 184; b) K. Takazawa, *Chem. Mater.* **2007**, *19*, 5293 – 5301; c) Y. S. Zhao, A. D. Peng, H. B. Fu, Y. Ma, J. N. Yao, *Adv. Mater.* **2008**, *20*, 1661 – 1665.

[15] a) R. Ben Chaabane, A. Ltaief, C. Dridi, H. Rahmouni, A. Bouazizi, H. Ben Ouada, *Thin Solid Films* **2003**, *427*, 371 – 376; b) A. R. Murphy, J. Liu, C. Luscombe, D. Kavulak, J. M. J. Frechet, R. J. Kline, M. D. McGehee, *Chem. Mater.* **2005**, *17*, 4892 – 4899.

[16] a) M. L. Tang, A. D. Reichardt, N. Miyaki, R. M. Stoltenberg, Z. Bao, *J. Am. Chem. Soc.* **2008**, *130*, 6064 – 6065; b) R. Capelli, F. Dinelli, S. Toffanin, F. Todescato, M. Murgia, M. Muccini, A. Facchetti, T. J. Marks, *J. Phys. Chem. C* **2008**, *112*, 12993 – 12999.

